Evidence for high-T_c ferromagnetism in $Zn_x(ZnO)_{1-x}$ granular films mediated by native point defects

X. Zhang,[1] Y. H. Cheng,[1] L. Y. Li,[1] Hui Liu,[1,*] X. Zuo,[1,†] G. H. Wen,[2] L. Li,[3] R. K. Zheng,[4,‡] and S. P. Ringer[4]
[1]*College of Information Technical Science, Nankai University, Tianjin 300071, China*
[2]*National Laboratory of Superhard Materials, Jilin University, Changchun 130012, China*
[3]*Institute of Material Physics, Tianjin University of Technology, Tianjin 300384, China*
[4]*Australian Key Center for Microscopy and Microanalysis, University of Sydney, Sydney, New South Wales 2006, Australia*
(Received 17 May 2009; revised manuscript received 4 November 2009; published 30 November 2009)

$Zn_x(ZnO)_{1-x}$ granular films with nominal atomic concentration of $x=0\sim1$ were prepared by magnetron cosputtering method. Ferromagnetism is observed in films with $0.04\leq x<0.60$. The room-temperature saturated magnetization increases with increasing x and reaches its maximum value of about 3.34 emu/cc at $x=0.31$. The temperature-dependent magnetization curve could be fitted within the framework of Stoner model in a large temperature range from 50 to 800 K. The obtained Curie temperature is higher than 500 °C. It is found that the main point defects in ZnO are Zn interstatial and oxygen vacancy. Room-temperature photoluminescence analysis and high-temperature x-ray diffraction measurement show conclusive evidence that the native point defect of Zn interstitial plays a crucial role in the observed magnetic behaviors. By implicating the shallow donor related carriers and/or extending the charge-transfer mechanism to metal/semiconductor heterostructure, the result could be qualitatively explained based on the Stoner theory of band magnetism. These findings may help to get further insight into the ferromagnetic origin in nonmagnetic ion doped ZnO systems.

DOI: 10.1103/PhysRevB.80.174427 PACS number(s): 75.50.Pp, 75.70.Cn, 75.50.Dd

I. INTRODUCTION

During the last decade, extensive studies have been carried out on ZnO-based diluted magnetic semiconductors (DMSs) due to their promising versatile applications such as spintronic, optoelectronic, and piezoelectric materials.[1,2] Theoretical works have predicted that high-T_c ferromagnetism should exist in transition-metal-doped ZnO systems. Several indirect exchange interactions models based on Heisenberg exchange coupling of localized spins, including Zener/Ruderman-Kittel-Kasuya-Yosida-type exchange, double- and superexchange, F-center-mediated bound magnetic polaron models have been invoked to explain the ferromagnetism in different type of DMSs.[3–6] On the contrary, experimental results are quite contradictory to each other. Room-temperature ferromagnetism has been found in transition-metal-doped ZnO-based DMSs.[4–14] However, there are still some reports indicating no sign of ferromagnetism.[15–17] Moreover, the well-known problem of transition-metal precipitates or clusters in ZnO may also be the origin of ferromagnetism.[18,19]

Despite the pitfalls associated with magnetic precipitates or clusters, careful measurements have yielded significant evidence which indicates that the point defects of ZnO, such as oxygen vacancy (V_O) or Zn interstitial (Zn_i), are crucial for ferromagnetism of transition-metal-doped ZnO.[7–14] The recent x-ray magnetic circular dichroism (XMCD) investigations by Tietze *et al.*[20] even showed that the doped Co atoms were paramagnetic in their ferromagnetic Co-doped ZnO films. Simultaneously, room-temperature ferromagnetism has also been found in undoped HfO_2, ZnO, and TiO_2 films or partially oxidized Zn nanowires, which was attributed to point defects.[21–23] These findings have provided conclusive evidence that the dopant cation of magnetic metal is not essential for ferromagnetism. It is the native point defects which play an important role in ferromagnetic origin.

Nevertheless, the chemistry of ZnO point defects is sophisticated. There is still no definite agreement on the nature of the defect-related ferromagnetism of ZnO-based DMSs. Both Zn_i and V_O are declared exclusively to be the magnetic origin.[7–14] Therefore, more delicate experimental investigations are needed to distinguish the different types of point defects and the observed magnetic property, and thus to identify the nature of the room-temperature ferromagnetism in nonmagnetic ion doped ZnO materials. In this paper, the structural, optical and magnetic properties of $Zn_x(ZnO)_{1-x}$ granular films are studied. The heteroelement free system provide an ideal research object for the identification of possible magnetic contributions from different types of native point defects. The magnetic measurements show that the films are ferromagnetic with a T_c above 500 °C. It is found that the point defect of Zn interstitial plays a crucial role in the observed magnetic behaviors. The ferromagnetism could be qualitative described based on the Stoner theory of band magnetism. These results may help to get a further insight into the ferromagnetic origin of nonmagnetic ion doped ZnO systems.

II. EXPERIMENTAL

$Zn_x(ZnO)_{1-x}$ granular films with atomic concentration of $x=0\sim1$ were fabricated by cosputtering pure ZnO and Zn targets in Ar and O_2 mixture (with 20:1 of Ar to O_2 flow rate) at ambient room temperature. The base pressure of the chamber was better than 1×10^{-5} Pa before deposition and the total pressure for sputtering was kept at 2.0 Pa. Glass and Kapton substrates were used for deposition. The substrate rotated at 30 rpm during the deposition and the distance from the targets to substrate was about 15 cm. The RF sputtering power of ZnO target was kept at 260 W. The composition of

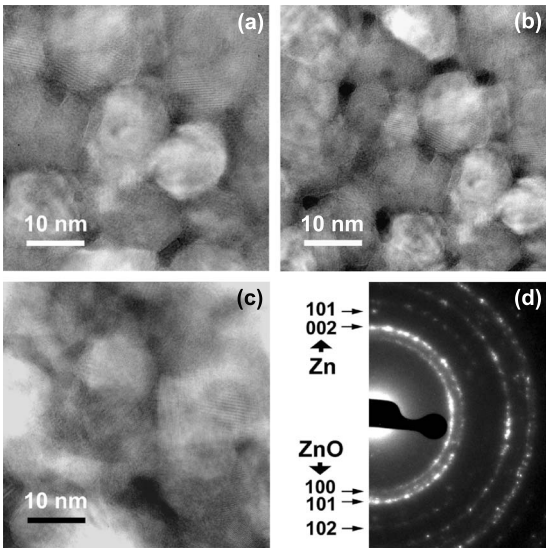

FIG. 1. Bright field TEM images of $Zn_x(ZnO)_{1-x}$ films with different x of (a) 0.07, (b) 0.24, and (c) 0.31. (d) SAED pattern of $Zn_{0.31}(ZnO)_{0.69}$ film.

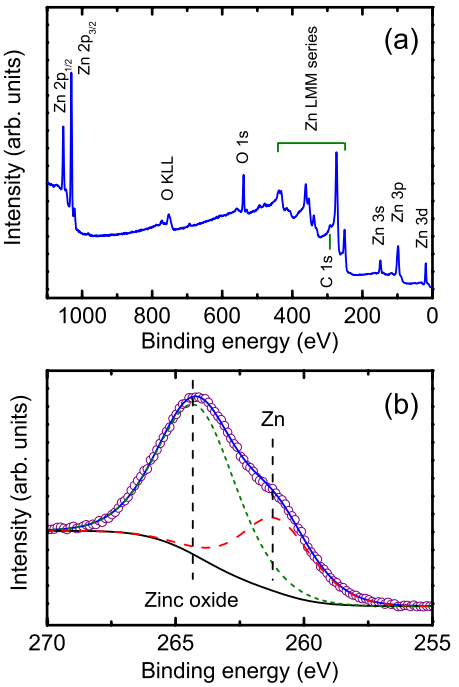

FIG. 2. (Color online) (a) XPS survey scan spectrum and (b) Zn LMM peaks of the $Zn_x(ZnO)_{1-x}$ film (x=0.31).

$Zn_x(ZnO)_{1-x}$ granular films was adjusted by changing the DC sputtering power applied on Zn target. The film thickness was kept around 100 nm. The magnetic properties at temperatures below 300 K were measured by a Quantum design physical property measurement system (PPMS-9). Magnetic measurements above 300 K were performed using a vibrating sample magnetometer (VSM). The microstructures of the samples were investigated by high-resolution transmission electron microscopy (TEM). The chemical states and compositions were analyzed by x-ray photoelectron spectroscopy (XPS). The temperature-dependent structural measurements were performed by x-ray diffraction (XRD) with the same heating rate, temperature range and duration as that of VSM measurement. Photoluminescence (PL) measurements were performed at room temperature with a 325 nm excited wavelength. The electrical transport properties were measured using an Accent HL-5550PC system.

III. RESULTS AND DISCUSSION

Presented in Fig. 1 are the high-resolution TEM images of $Zn_x(ZnO)_{1-x}$ films. It can be seen that the nanocrystalline ZnO or Zn granules are well separated by grain boundaries. The average grain diameter is estimated to be around 12 nm. All diffraction rings (only the SAED pattern for x=0.31 is presented in Fig. 3) can be indexed into polycrystalline hexagonal ZnO or Zn. However, the diffraction spots corresponding to metallic Zn are scarce and weak, which may be due to the large amount of Zn_i presented in ZnO lattice as indicated by the PL spectra discussed below.

In order to eliminate other possible magnetic contaminations, XPS measurements were performed to identify the elements and their chemical states in samples. Figure 2(a) shows a typical broad scan survey spectrum of the $Zn_{0.31}(ZnO)_{0.69}$ film taken at $h\nu$=1253.6 eV. The photoelectron peaks of the main elements, Zn, O and C, and Auger Zn LMM and O KLL peaks, were obtained. No other detectable contaminated element (above 0.1%) exists in the $Zn_x(ZnO)_{1-x}$ films. The presence of Zn in the films was also confirmed by AES signal in XPS spectrum. Figure 2(b) presents a $Zn(L_3M_{45}M_{45})$ AES signal for the $Zn_{0.31}(ZnO)_{0.69}$ film. The major peak locates at 264.2 eV is considered to be associated with Zn LMM in ZnO. The minor one at 261.2 eV is due to Zn(LMM) of metallic Zn or Zn_i in ZnO lattice.[24]

Figure 3(a) illustrates the room-temperature magnetization loops of the $Zn_x(ZnO)_{1-x}$ films. In order to compare the curves with that of pure Zn and ZnO, the diamagnetic background signal is not deduced. It can be seen that the samples are ferromagnetic with clear hysteresis behaviors, which is reproducible within the experimental conditions. However, the as-deposited pure Zn and ZnO films are diamagnetic, confirming that no ferromagnetic impurities were introduced during the preparation of the films. Figure 3(b) presents the dependence of the magnetic moment of $Zn_x(ZnO)_{1-x}$ films on the atomic concentration x at 300 K. It can be seen that, the films are nonferromagnetic at $x<0.04$ and $x \geq 0.60$. As $x \geq 0.04$, the magnetic moment increases with increasing x and reaches its maximum value of about 3.34 emu/cc at x=0.31. Then the moment decreases with increasing x, showing a strong dependence on x. To further investigate the ferromagnetic properties of $Zn_x(ZnO)_{1-x}$ films, high-temperature hysteresis loops were measured as shown in Fig. 3(c). The sample shows ferromagnetic behavior and the saturated magnetization decreases with increasing temperature. The obtained T_c is higher than 500 °C, which is in accordance with the fitting parameter of T_c(=800 K) presented in Fig. 7 below.

In the previous studies on ZnO-based DMSs, accumulated evidence indicates that Zn_i and V_O play a crucial role in

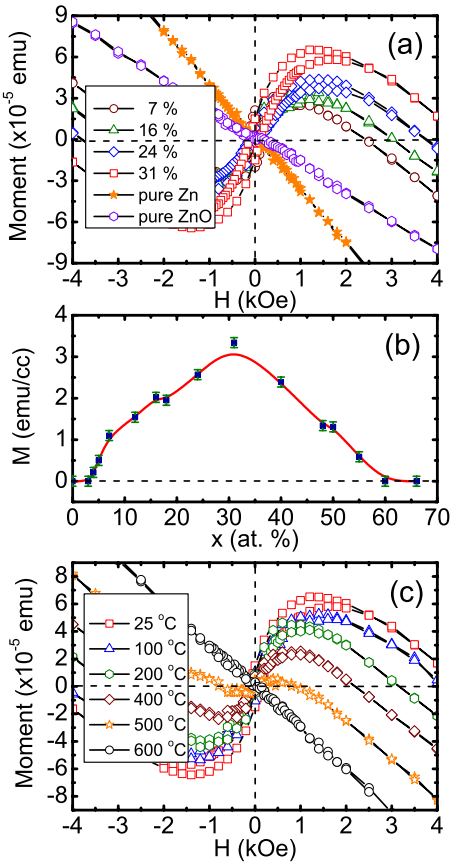

FIG. 3. (Color online) (a) Magnetization curves of the $Zn_x(ZnO)_{1-x}$ films with different x at 300 K; (b) the saturated magnetization versus x at 300 K; and (c) hysteresis loops for the sample with $x=0.31$ at different temperatures. The diamagnetic background signals in (a) and (c) are not deduced. The solid red line in (b) is a guide to eyes.

generating the ferromagnetism.[7–14] However, the detailed mechanism is unclear yet. One of the important obstacles is that the chemistry of ZnO defect is sophisticated, including the main defect types of Zn_i, Zn vacancy, oxygen interstitial and V_O. It is known that PL is a useful tool for the investigation of intrinsic point defects in ZnO.[25] Fig. 4 shows the experimental and Gaussian fitting data for the room-temperature PL spectra of $Zn_x(ZnO)_{1-x}$ films. As there is still no definite agreement on the origins and positions of the visible emission of ZnO, the donor levels of point defects used in the Gaussian fitting are based on the recent reports of ZnO.[25,26] It can be seen that the main point defects in the $Zn_x(ZnO)_{1-x}$ films are Zn_i and V_O, which is in accordance with the reported experimental results where Zn_i and V_O are the predominant native point defects in ZnO.[1] In pure ZnO film, the defect peaks are fairly weak compared with that of $Zn_x(ZnO)_{1-x}$ films ($x \geq 0.07$). However, while the area of V_O is nearly stable with $x \geq 0.07$, the amount of Zn_i increases severely with x. Two possible mechanisms may be responsible for the increase of Zn_i. The first one is due to the cosputtering Zn and ZnO process which would bring more Zn_i into ZnO lattice. On the other hand, it has been demonstrated that the diffusion barrier for Zn_i is low, which makes it become mobile at temperature as low as 130 K.[27] Therefore, the second reason may come from the diffusion effect of metal Zn in films, which is similar to the reported Zn-metal-vapor diffusion process.[10,11]

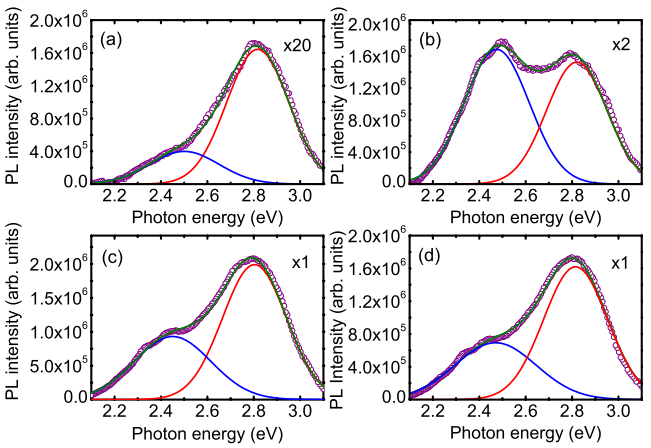

FIG. 4. (Color online) Fitting and experimental data for room-temperature PL spectra of $Zn_x(ZnO)_{1-x}$ films with different x of (a) 0, (b) 0.07, (c) 0.24, and (d) 0.31. The solid red and blue lines are Gaussian fitting of Zn_i(~2.82 eV) and V_O(~2.47 eV), respectively.

In order to further determine the relations between the main point defects (*i.e.*, Zn_i and V_O in these films) and magnetization, the defect-related high-temperature structural properties were also measured. However, the PL cannot be operated at high temperature as its peaks are broad and overlap with each other. On the other hand, due to the dynamic diffusion effect of Zn_i into and out of ZnO lattice at high temperature (above 500 °C), the PL spectra which can only be operated below room temperature cannot resemble the dynamic process of Zn_i. Recently, Judith *et al.*[11] established a close correlation between the lattice constant along the c axis and Zn_i level in pure or doped ZnO, where the c parameter changes as a result of a decrease or increase in Zn_i concentration. They also demonstrated that, under the low-temperature annealing conditions (~500 °C for 3 h), the oxygen annealing atmosphere and growth defects (such as dislocations and atomic disorder) do not influence c parameter. Their findings established a way to discriminate the lattice variations arising from Zn_i and V_O, which are the two most important point defects related to ferromagnetism in ZnO-based DMSs. Shown in Fig. 5 are the XRD spectra of $Zn_{0.31}(ZnO)_{0.69}$ film at different temperatures with the same heating rate, temperature range and duration as that of VSM measurements. It can be seen that the film are highly oriented with preferential growth along ZnO (002). However, the diffraction pattern of Zn is quite week due to the relatively low concentration of Zn granules, which is in accordance with the result of TEM. The inset to Fig. 5 shows the detailed position of the (002) peaks which shifts toward higher angle when temperature increases.

In order to show the relation between point defects and the ferromagnetic property more clearly, the areas of the Gaussian fitting peaks in the PL spectra and the room-temperature saturated magnetization with different x are presented in Fig. 6(a). It can be seen that, while V_O keeps steady

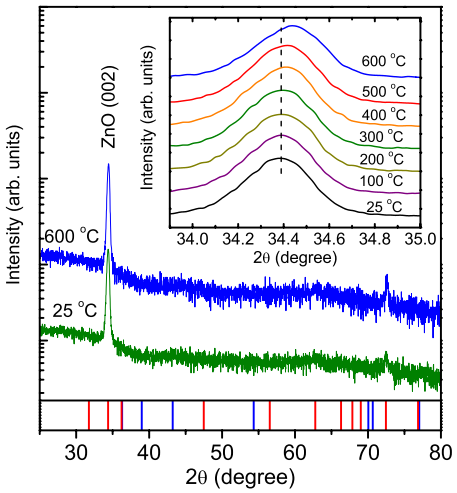

FIG. 5. (Color online) XRD patterns of $Zn_x(ZnO)_{1-x}$ film ($x=0.31$) film at different temperatures. Inset: Change in lattice parameter compared to pure zinc oxide. Also shown in the figure are the standard diffraction positions of hexagonal ZnO and Zn.

at $x \geq 0.07$, there is a direct correlation between the saturated magnetization and the concentration of Zn_i. In Fig. 6(b), the corresponding c axial parameter determined from the full width at half maximum of ZnO (002) peak decreases with increasing temperature and a severely drop trend is observed above 400 °C. The decrease of c parameter with temperature is similar to the result presented by Judith *et al.*,[11] which results from the leakage of Zn_i out of ZnO lattice, except that the variation of out-of-plane cell parameter c ($\sim$0.008 Å) is two times larger in this study. This may be due to the cosputtering process of Zn and ZnO, a smaller granule size in films

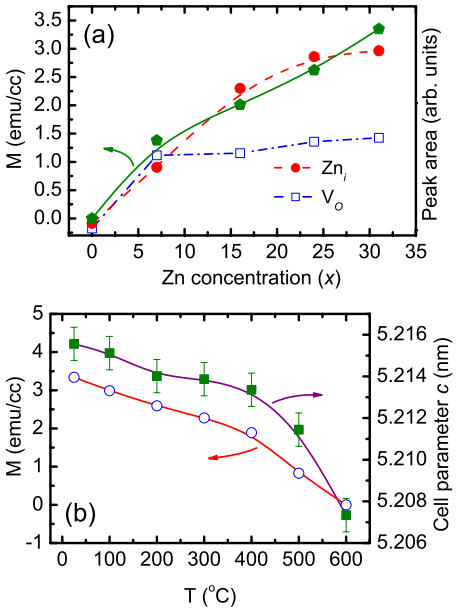

FIG. 6. (Color online) (a) Variation of room-temperature magnetization and PL peak areas of Zn_i and V_O in $Zn_x(ZnO)_{1-x}$ films with different concentrations. (b) Variation of cell parameter c and saturated magnetization of $Zn_x(ZnO)_{1-x}$($x=0.31$) film at different temperatures.

and a higher process temperature (600 °C). Since the large variation in c, determination of this parameter is a useful diagnostic tool for the qualitative relation between ferromagnetism and Zn_i concentration. The correlation, provided both from room-temperature PL analysis and high-temperature XRD measurement shown in Fig. 6, provides conclusive evidence that Zn_i plays an important role in the ferromagnetism in $Zn_x(ZnO)_{1-x}$ films. Nevertheless, Zn_i cannot carry magnetic moment as its d orbits are fully occupied by electrons. It is important to mention that there is no ferromagnetic signal in pure ZnO films even with certain amount of Zn_i as indicated in Fig. 3 and 4. On the other hand, there is still no report on the ferromagnetism originated from Zn_i based on theoretical calculations.

Very recently, Coey *et al.*[13] and Peng *et al.*[28] proposed a qualitative model based on the Stoner theory of band magnetism, where the impurities shift the Fermi level (E_F) to a peak in the local density of states due to the defect states and the Stoner criterion for ferromagnetism can be satisfied. Based on this scenario, the dopants in DMSs play no essential role in carrying magnetic moment. By implicating the shallow donor (such as Zn_i) related carriers,[13] the result could be qualitatively described by Stoner theory of band magnetism. In defective $Zn_x(ZnO)_{1-x}$ films, the point defects such as Zn_i (and/or V_O, or their complex) form an impurity band right below the bottom of the conduction band (i.e., $\sim$3.3 eV) as indicated in Fig. 4. However, in pure ZnO films ($x=0$), the low concentration of Zn_i and V_O is not sufficient to induce ferromagnetism. By cosputtering Zn and ZnO process, more Zn_i are introduced into the ZnO lattice which would bring more electrons to the defect states. On the other hand, with the present of metal Zn, Zn/ZnO heterostructure would form. The possible charge transfer from metallic Zn to n-type ZnO might take place. As the work functions of Zn and n-type ZnO are 4.3 and 5.2$\sim$5.4 eV respectively,[29,30] the electrons in Zn will diffuse into the impurity band of ZnO to establish a constant E_F level for both sides, which would further increases the electrons in defect states. Spontaneous ferromagnetism occurs when it satisfies the Stoner Criterion: $D(E_F)J>1$, where $D(E_F)$ is the density of state at E_F, and J represents the strength of the exchange interaction, as in the case with $x \geq 0.07$. More Zn_i (Fig. 4) and metal Zn would form in $Zn_x(ZnO)_{1-x}$ films with increasing x, and therefore, enhances magnetization as indicated in Fig. 6(a).

Historically, the Stoner model was proposed around 1930s,[31–34] which is based on the band theory of electrons in solids and regards magnetic carriers as itinerant or Bloch electrons. Considerable improvement of the Stoner model has been achieved by Moriya *et al.*[35,36] through the inclusion of the spin-fluctuation effects within the framework of self-consistent renormalization theory. Lately, Lonzarich and Taillefer provided a refined version of Stoner model based on Moriya's theory, which proposed a better quantitative description of the experimental results for weak itinerant ferromagnetism.[37] According to this theory, the contributions to magnetization include spin-wave excitations, single-particle (SP) excitations, and local spin-density fluctuations (LSFs) depending on temperatures. For temperatures close to T_c, the local spin-density fluctuations alone contribute to $M(T)$,[37]

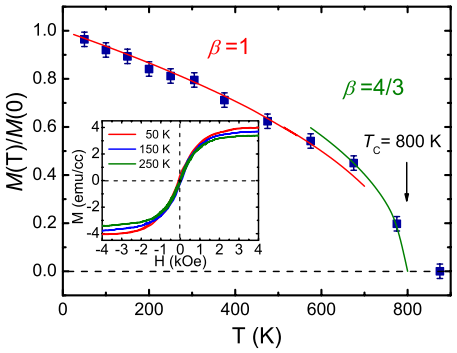

FIG. 7. (Color online) Temperature dependence of the saturated magnetization of $Zn_x(ZnO)_{1-x}$ film with $x=0.31$ and $M(0)=4.2$ emu/cc. The solid red and green lines are the fitting curves of $M(T)/M(0)=[1-(T/T_c)^{\beta}]^{1/2}$ with $\beta=1$ and 4/3, respectively. The inset presents magnetization hysteresis loops at low temperatures.

$$[M(T)/M(0)]_{LSF}=[1-(T/T_c)^{4/3}]^{1/2}. \quad (1)$$

For a wide range of intermediate temperatures, the magnetization can be described by the equation[37] of

$$[M(T)/M(0)]_{SP+LSF}=[1-(T/T_c)]^{1/2}. \quad (2)$$

The temperature dependence of magnetization in different temperature ranges predicted by Eqs. (1) and (2) has indeed been observed in a number of weak itinerant ferromagnets.[38] In order to get a further insight into the magnetic mechanism of the granular $Zn_x(ZnO)_{1-x}$ films, the low-temperature magnetic loops for $x=0.31$ were also measured. Figure 7 shows the temperature dependence of the saturated magnetization of $Zn_x(ZnO)_{1-x}$ film with $x=0.31$. It can be seen that the magnetization curve could be fitted well by Eq. (2) in a large temperature range of 50~600 K, which indicates that the magnetization comes from the combination effect of single-particle excitations and local spin-density fluctuations. At temperatures higher than 600 K, the magnetization is contributed from the local spin-density fluctuations and can be described by Eq. (1). Furthermore, the fitting parameter of T_c(=800 K) is consistent with the Curie temperature obtained from the experimental results shown in Figs. 3(c) and 6(b).

The electrical measurements indicate that the $Zn_x(ZnO)_{1-x}$ ($x=0\sim0.60$) films are highly insulating with a sheet resistance higher than 10^{11} Ω/sq, which value is near our experimental extreme. Thus the resistivity is larger than 10^6 Ω cm considering the thickness of about 100 nm, which may be due to the oxygen atmosphere during deposition. The dielectric state of the $Zn_x(ZnO)_{1-x}$ films is similar to most reported results of doped or undoped ZnO samples and indicates that the defect regions are not sufficient to form a continuously conducting path. Therefore, the dielectric property of the whole sample could not rule out the possibility of carrier mediated ferromagnetism in the ferromagnetic regions.[4]

The possible charge-transfer effect from nanosized metal to *n*-type ZnO, and the metal-semiconductor junction model have been widely studied previously (for example, Ref. 39). The above mentioned Stoner theory of band magnetism has also been used for the explanation of ferromagnetism in defect-related DMSs.[13,28] However, it should be mentioned that the defect chemistry of ZnO is very complex and the model of Stoner theory of band magnetism needs to be quantitatively verified.[13] For example, the carrier concentration, the possible spin polarization, and the contributions of the metal/semiconductor interface to the ferromagnetism need to be clarified. Nevertheless, the speculation at the moment may open new perspectives and solution approaches for the puzzling field of ferromagnetism in nonmagnetic ion doped ZnO.

IV. CONCLUSIONS

In conclusion, room-temperature ferromagnetism is observed in $Zn_x(ZnO)_{1-x}$ granular films with $0.04\leq x<0.60$. The obtained T_c is higher than 500 °C. It is found that the main point defects in ZnO are Zn_i and V_O. Room-temperature photoluminescence analysis and high-temperature x-ray diffraction measurement show conclusive evidence that the native point defect of Zn_i plays a crucial role in the observed magnetic behaviors. The results could be qualitatively explained based on the Stoner theory of band magnetism. These findings may help to get further insight into the ferromagnetic origin in nonmagnetic ion doped ZnO systems.

ACKNOWLEDGMENT

The work described in this paper is supported by National Hi-tech (R&D) project of China (Project No. 2006AA03Z305).

*liuhui@nankai.edu.cn
†xzuo@nankai.edu.cn
‡r.zheng@usyd.edu.au

[1] S. Dutta, S. Chattopadhyay, A. Sarkar, M. Chakrabarti, D. Sanyal, and D. Jana, Prog. Mater. Sci. **54**, 89 (2009).
[2] F. Pan, C. Song, X. J. Liu, Y. C. Yang, and F. Zeng, Mater. Sci. Eng. R. **62**, 1 (2008).
[3] T. Dietl, H. Ohno, F. Matsukura, J. Cibert, and D. Ferrand, Science **287**, 1019 (2000).
[4] K. R. Kittilstved, W. K. Liu, and D. R. Gamelin, Nature Mater. **5**, 291 (2006).
[5] M. H. F. Sluiter, Y. Kawazoe, P. Sharma, A. Inoue, A. R. Raju, C. Rout, and U. V. Waghmare, Phys. Rev. Lett. **94**, 187204 (2005).
[6] J. M. D. Coey, M. Venkatesan, and C. B. Fitzgerald, Nature Mater. **4**, 173 (2005).
[7] E. Biegger, M. Fonin, U. Rüdiger, N. Janßen, M. Beyer, T. Thomay, R. Bratschitsch, and Y. S. Dedkov, J. Appl. Phys. **101**,

073904 (2007).
[8] N. H. Hong, J. Sakai, N. T. Huong, N. Poirot, and A. Ruyter, Phys. Rev. B **72**, 045336 (2005).
[9] K. R. Kittilstved, D. A. Schwartz, A. C. Tuan, S. M. Heald, S. A. Chambers, and D. R. Gamelin, Phys. Rev. Lett. **97**, 037203 (2006).
[10] D. A. Schwartz and D. R. Gamelin, Adv. Mater. **16**, 2115 (2004).
[11] J. L. MacManus-Driscoll, N. Khare, Y. Liu, and M. E. Vickers, Adv. Mater. **19**, 2925 (2007).
[12] X. Zhang, W. H. Wang, L. Y. Li, Y. H. Cheng, X. G. Luo, Hui Liu, Z. Q. Li, R. K. Zheng, and S. P. Ringer, Europhys. Lett. **84**, 27005 (2008).
[13] J. M. D. Coey and S. A. Chambers, MRS Bull. **33**, 1053 (2008); J. M. D. Coey, K. Wongsaprom, J. Alaria, and M. Venkatesan, J. Phys. D **41**, 134012 (2008).
[14] B. B. Straumal, A. A. Mazilkin, S. G. Protasova, A. A. Myatiev, P. B. Straumal, G. Schütz, P. A. van Aken, E. Goering, and B. Baretzky, Phys. Rev. B **79**, 205206 (2009).
[15] M. Bouloudenine, N. Viart, S. Colis, J. Kortus, and A. Dinia, Appl. Phys. Lett. **87**, 052501 (2005).
[16] S. Yin, M. X. Xu, L. Yang, J. F. Liu, H. Rösner, H. Hahn, H. Gleiter, D. Schild, S. Doyle, T. Liu, T. D. Hu, E. Takayama-Muromachi, and J. Z. Jiang, Phys. Rev. B **73**, 224408 (2006).
[17] W. Li, Q. Q. Kang, Z. Lin, W. S. Chu, D. L. Chen, Z. Y. Wu, Y. Yan, D. G. Chen, and F. Huang, Appl. Phys. Lett. **89**, 112507 (2006).
[18] J. H. Park, M. G. Kim, H. M. Jang, S. Ryu, and Y. M. Kim, Appl. Phys. Lett. **84**, 1338 (2004).
[19] S. Deka, R. Pasricha, and P. A. Joy, Phys. Rev. B **74**, 033201 (2006).
[20] T. Tietze, M. Gacic, G. Schütz, G. Jakob, S. Brück, and E. Goering, New J. Phys. **10**, 055009 (2008).
[21] M. Venkatesan, C. B. Fitzgerald, and J. M. D. Coey, Nature (London) **430**, 630 (2004).
[22] N. H. Hong, J. Sakai, and V. Brizé, J. Phys.: Condens. Matter **19**, 036219 (2007).
[23] J. B. Yi, H. Pan, J. Y. Lin, J. Ding, Y. P. Feng, S. Thongmee, T. Liu, H. Gong, and L. Wang, Adv. Mater. **20**, 1170 (2008).
[24] Y. Natsume and H. Sakata, Mater. Chem. Phys. **78**, 170 (2003).
[25] A. B. Djurišić and Y. H. Leung, Small **2**, 944 (2006).
[26] T. Moe Børseth, B. G. Svensson, A. Yu Kuznetsov, P. Klason, Q. X. Zhao, and M. Willander, Appl. Phys. Lett. **89**, 262112 (2006).
[27] P. Erhart and K. Albe, Appl. Phys. Lett. **88**, 201918 (2006).
[28] H. W. Peng, H. J. Xiang, S. H. Wei, S. S. Li, J. B. Xia, and J. B. Li, Phys. Rev. Lett. **102**, 017201 (2009).
[29] X. D. Bai, E. G. Wang, P. X. Gao, and Z. L. Wang, Nano Lett. **3**, 1147 (2003).
[30] Y. W. Zhu, H. Z. Zhang, X. C. Sun, S. Q. Feng, J. Xu, Q. Zhao, B. Xiang, R. M. Wang, and D. P. Yu, Appl. Phys. Lett. **83**, 144 (2003).
[31] F. Bloch, Z. Phys. **57**, 545 (1929).
[32] N. F. Mott, Proc. Phys. Math. Soc. Jpn. **47**, 571 (1935).
[33] J. C. Slater, Phys. Rev. **49**, 537 (1936).
[34] E. C. Stoner, Proc. R. Soc. London, Ser. A **154**, 656 (1936).
[35] T. Moriya and A. Kawabata, J. Phys. Soc. Jpn. **34**, 639 (1973).
[36] T. Moriya, J. Magn. Magn. Mater. **31-34**, 10 (1983).
[37] G. G. Lonzarich and L. Taillefer, J. Phys. C **18**, 4339 (1985).
[38] P. D. Babu, Ph.D. thesis, University of Hyderabad, 1995.
[39] X. D. Wang, C. J. Summers, and Z. L. Wang, Appl. Phys. Lett. **86**, 013111 (2005).